*J Physiol* 587.3 (2009) pp 521–529



The Journal of Physiology

# NKCC1 (SLC12a2) induces a secondary axis in *Xenopus laevis* embryos independently of its co-transporter function

Zoë S. Walters, Kim E. Haworth and Branko V. Latinkic

*Cardiff School of Bioscience, Cardiff University, Museum Avenue, Cardiff CF10 3AX, UK*

**NKCC1 is a broadly expressed $Na^+$–$K^+$–$Cl^-$ co-transporter involved in regulation of ion flux across the cell membrane and in regulating cell volume. Whilst much is known about the co-transporter activity of NKCC1 and its regulation by protein kinases and phosphatases, little is known about the activities of NKCC1 that are co-transporter independent. In this report we show that over-expression of NKCC1 in embryos of *Xenopus laevis* induces secondary axes, independently of its co-transporter activity. In addition, over-expression of NKCC1 results in the formation of neural tissue in ectodermal explants. We also show that NKCC1 is expressed broadly but non-uniformly in embryos of *Xenopus laevis* and *Xenopus tropicalis*, with prominent expression in the notochord, nervous system and stomach. These results provide insights into an additional, previously unreported activity of NKCCl.**

(Received 14 August 2008; accepted after revision 28 November 2008; first published online 1 December 2008)
**Corresponding author** B. V. Latinkic: Cardiff School of Bioscience, Cardiff University, Museum Avenue, Cardiff CF10 3AX, UK. Email: latinkicb@cardiff.ac.uk

The SLC12 solute carriers were first identified in fish and subsequently in mammals (Gamba *et al.* 1993, 1994; Xu *et al.* 1994). Family members consist of electro-neutral ion transporters that co-transport potassium, sodium and chloride ions. SLC12A1–3 are transporters of sodium, potassium and chloride ions and SLC12A4–7 are potassium chloride transporters (reviewed in Hebert *et al.* 2004). In this report we describe our studies of SLC12a2 (also called NKCC1), a $Na^+$–$K^+$–$Cl^-$ co-transporter. NKCC1 is located in the basolateral membrane of epithelial cells and has been shown to regulate the flux of chloride ions (Hebert *et al.* 2004). In non-epithelial cells there is evidence to suggest that NKCC1 is involved in the regulation of cell volume (Lytle, 1997; Hebert *et al.* 2004). Human NKCC1 protein contains 1166 amino acids and 12 transmembrane domains, which are flanked by hydrophilic amino- and carboxy-terminal domains. The N-terminus contains an RVXFXD domain that is involved in binding protein phosphatase type I, and a (R/K)FX(V/I) domain thought to bind stress-related protein kinases (Darman *et al.* 2001; Piechotta *et al.* 2002). Payne & Forbush (1995) predicted two sites for N-glycosylation on the extracellular loop between transmembrane domains 7 and 8, and also a potential phosphorylation site in the cytoplasmic C-terminal region.

Mouse NKCC1 protein shares 93% sequence identity with human NKCC1 (Payne & Forbush, 1995). Expression studies have shown mouse NKCCl to be localized broadly in the developing mouse embryo, including prominent expression in secretory epithelia, muscle cells, neurones and red blood cells. Mutations in mouse NKCC1 result in inner ear defects and consequently deafness (Delpire *et al.* 1999). NKCC1 null mice are also hypotensive, consistent with the findings of numerous reports that have implicated NKCC1 in hypertension (Gimenez, 2006; Garg *et al.* 2007; Flatman, 2008).

The transporter activity of NKCC1 is regulated by phosphorylation and in response to osmotic stress and cell shrinkage (Flatman, 2002; Hebert *et al.* 2004; Gamba, 2005). NKCC1 activity is regulated by several serine/threonine kinases, including PKC, myosin light chain kinase (MLCK), extracellular signal-regulated kinase (ERK) and PKA. PKC and ERK regulate NKCC1 in epithelial cells in response to hyperosmot ic stress (Liedtke & Cole, 2002). The ion transporter function of NKCCl is relatively well documented but its additional roles are virtually unknown. One exception is a study which has implicated NKCC1 in the activation of ERK signalling in the Balb/c3T3 cell line (Panet *et al.* 2006).

In this report, we provide evidence for additional activity of NKCC1, by showing that it can induce a secondary axis in *Xenopus* embryos independently of its co-transporter activity.

## Methods

### *Xenopus* embryos

*Xenopus* embryos were obtained by both *in vitro* fertilization and natural mating following standard



DOI: 10.1113/jphysiol.2008.161562

procedures (Sive *et al.* 2000). *X. laevis* embryos were de-jellied in 2.2% cysteine in water. *X. tropicalis* embryos were de-jellied in 3% cysteine in 11% Marc's Modified Ringer solution (MMR) (Sive *et al.* 2000). *X. laevis* embryos were cultured in 10% normal amphibian medium (NAM; 100% NAM is 110 mM NaCl, 2 mM KCl, 1 mM $Ca(NO_3)_2$, 1 mM $MgSO_4$, 0.1 mM EDTA and 2 mM sodium phosphate, pH 7.4 (Sive *et al.* 2000)), and *X. tropicalis* embryos were cultured long-term in 5% MMR (*Xenopus* embryos require hypotonic media for normal development). Staging of embryos was carried out according to Nieuwkoop & Faber (1994).

For over-expression experiments, *X. laevis* embryos were injected in one ventral blastomere at the four-cell stage in 75% NAM with 3% Ficoll and left to heal for 2 h (Sive *et al.* 2000). These iso-tonic and -osmotic conditions are standard and are used to prevent cytoplasmic leakage during microinjections (Sive *et al.* 2000). For secondary axis formation assay, the embryos were subsequently cultured in 10% NAM until stage 35, as normal early development of *Xenopus* embryos requires hypotonic environment. Animal caps were explanted at stage 9 and were cultured in 75% NAM. Animal cap explants were treated with 0.1 or 0.3 M LiCl in 75% NAM for 5 or 10 min, respectively, and were cultured in 75% NAM until sibling control embryos reached stage 10.5.

**Inhibitor treatment.** Bumetanide (Sigma) was added to 10% normal amphibian medium (NAM) within the range of 5 $\mu$M to 15 $\mu$M and also 700 $\mu$M to 1100 $\mu$M and embryos were cultured in this medium up to stage 35. Furosemide (Sigma) was added to 10% NAM within the range of 0.5 mM to 3 mM, and embryos were cultured in this medium up to stage 35. Comparable results were obtained when inhibitors were present between stages 6–10 and stages 10–35.

**Ion replacement.** The sodium ion replacement media based on MMR was made up using choline chloride (100 mM choline chloride, 2 mM KCl, 1 mM $MgSO_4$, 2 mM $CaCl_2$, 5 mM Hepes, pH 7.8). To reduce chloride ion concentration media was made up using isethionic acid (100 mM isethionic acid, 2 mM KCl, 1 mM $MgSO_4$, 2 mM $CaCl_2$, 5 mM Hepes, pH 7.8). Embryos were injected in 75% MMR with 3% Ficoll and left to heal for 2–3 h. Embryos were washed several times in replacement media and were incubated in the same media until stage 35.

## Molecular biology

**Cloning.** PCR primers were designed to the *X. tropicalis* full length NKCC1 clone (IMAGE: 7548644; RZPD, Germany) to encompass 410 amino acids in frame from the start codon, and to include all 11 transmembrane domains (1–751 NKCC1). The forward primer contained a 5′-tail with a *Not*I site, and the reverse primer contained a 5′-tail with a *Sal*I site for directional cloning into pCS107 expression vector. NKCC1 1–751 primers were as follows: 5′-TCAGCGGCCGCAACTGACCACAGCACATGGA-3′ and 5′-AGTCAGCTGATTCAAAGCTGGACGTGAATTT GG-3′. PCR was carried out using Phusion High-Fidelity DNA Polymerase (NEB) and the sequence of the resulting product was verified.

***In vitro* transcription of mRNA.** The original clone of NKCC1 isolated in secondary axis expression screen is TEgg088e14, sequence accession number CR761200.

Capped mRNA for injection of all NKCC1 variants used in this study was made using *Asc*I-linearized templates and SP6 polymerase (NEB) and 7mG(ppp)G RNA Cap Structure Analog (NEB), according to standard protocols (Sive *et al.* 2000). Dominant-negative *Xenopus* Tcf3 ($\Delta$Tcf3) was described by (Molenaar *et al.* 1996) as a version of Tcf3 (X99309) that lacks the first 32 amino acids. It was transcribed from a *Xba*I-linearized template by T7 polymerase.

## Immunohistochemistry

*X. laevis* embryos injected with NKCC1 into one ventral cell at the four-cell stage were cultured up to stage 30 and were processed for immunohistochemistry as previously described (Sive *et al.* 2000). 12/101 antibody, a marker of skeletal muscle directed against a 102 kDa skeletal muscle protein (Developmental Studies Hybridoma Bank) (Kintner & Brockes, 1984), was used at a 1 : 100 dilution, and goat anti-mouse horseradish peroxidase-conjugated secondary antibody (Chemicon) at a 1 : 500 dilution. Colour was developed using diaminobenzidine (DAB) substrate (Sigma).

## Whole-mount *in situ* hybridization

Whole-mount *in situ* hybridization was carried out as previously described (Sive *et al.* 2000). A digoxigenin (Roche)-labelled antisense RNA probe was generated from full length *Xenopus tropicalis* NKCC1 cDNA using T7 polymerase following linearization with *Hind*III. Colour reactions were performed using BM purple alkaline phosphatase substrate (Roche). Embryos for sectioning were embedded in paraffin and processed for routine histology.

## RT-PCR

Total RNA was extracted from at least 30 animal cap explants per sample by the guanidinium isothyocyanate method (Chomczynski & Sacchi,

1987) and was used to generate cDNA using random primers (Promega) and MMLV reverse transcriptase (Invitrogen), according to manufacturer's recommendations. cDNA was verified by PCR using ornithine decarboxylase (ODC) primers: forward 5′-GCCATTGTGAAGACTCTCTCCATTC and reverse 5′-TTCGGGTGATTCCTTGCCAC. Other primers were as follows: XAG: forward 5′-CTGACTGTCCGATCAGAC and reverse 5′-GAGTTGCTTCTCTGGCAT; N-tubulin: forward 5′-ACACGGCATTGATCCTACAG and reverse 5′-AGCTCCTTCGGTGTAATGAC; *Siamois*: forward 5′-AAGGAACCCCACCAGGATAA and reverse 5′-CTGGTACTGGTGGCTGGAGA.

## Results

### *Xenopus* NKCC1

The *Xenopus tropicalis* NKCC1 sequence was isolated during an expression screen for genes with secondary axis-inducing capabilities using a *Xenopus tropicalis* full length expression cDNA library (Gilchrist *et al.* 2004). Sequence comparisons show that the *Xenopus tropicalis* NKCCl protein has 96% protein sequence identity with *Xenopus laevis* NKCC1 (GenBank accession ABN05233). The *Xenopus tropicalis* NKCC1 gene has an open reading frame of 3483 bp and codes for a protein of 1161 amino acids with 74%, 80% and 84% sequence identity with human (GenBank accession AAH33003), mouse (GenBank accession AAC77832) and chick (ENSGALP00000023629) NKCC1, respectively.

*Xenopus* NKCC1 is an 11 transmembrane (TM) domain protein that lacks the last TM domain found in the human form of the protein. Both the N-terminal RVXFXD and (R/K)FX(V/I) domains present in the human NKCC1 protein are also present in the *Xenopus* protein. In the genome of *X. tropicalis* NKCC1 is found on scaffold 7 and is flanked at the 3′ end by fibrillin 2 and solute carrier family 27 member 2. This region of the *X. tropicalis* genome has its syntenic counterparts on the mouse and human chromosomes 18 and 5, respectively (www.metazome.net).

### Expression of NKCC1 in *Xenopus* embryos

The expression pattern of *Xenopus* NKCC1 was examined by whole-mount *in situ* hybridization (Fig. 1). Maternal NKCC1 mRNA is observed at the animal pole in all cleavage stage embryos (Fig. 1*A*). At gastrula stages NKCC1 expression is widespread but absent from the vegetal pole (presumptive endoderm; Fig. 1*B*). By stage 19 the pattern of expression of NKCC1 is more defined and NKCC1 transcripts are found at high levels in the notochord, with lower levels of expression in the developing nervous system (Fig. 1*C–E*). Throughout neurula and early tadpole stages NKCC1 continues to be strongly expressed in the brain regions and neural tube (data not shown). In early tadpoles (stage 35), NKCC1 is expressed in the eye, otic vesicle, branchial arches and forebrain (Fig. 1*G*). At stage 42, NKCC1 transcript expression is still present in the otic vesicle and branchial arches but additional gut expression is observed (Fig. 1*H*). As the development of the gut proceeds through coiling and regional differentiation, NKCC1 expression becomes restricted to the stomach, as shown by *in situ* hybridization on dissected guts of stage 54 *X. tropicalis* and *X. laevis* embyos (Fig. 1*I* and *J*). The expression pattern of NKCC1 in *X. laevis* and *X. tropicalis* was the same throughout embryonic development, as expected for closely related members of the same genus (data not shown).

### NKCC1 over-expression induces secondary axis formation in *Xenopus laevis* embryos

Initially a truncated form of NKCC1 consisting only of the C-terminus of the protein containing amino acids 1079–1166 (1079–1166 NKCC1), was identified for its secondary axis-inducing capability (accession number CR761200). Injection of 2–4 ng of this mRNA into one ventral cell of a four-cell embryo induced partial secondary axis (48%; $n = 87$) (Fig. 2). When tested for secondary axis induction, a lower dose (800 pg) of the full length NKCC1 (FL NKCC1) was sufficient to induce partial secondary axis induction in 45% of injected embryos ($n = 87$; Fig. 2).

To test whether the C-terminus fragment 1079–1166 of NKCC1, which is sufficient for secondary axis induction, is also required for activity of the full length NKCC1, we tested a construct that lacked the C-terminus but retained all 11 transmembrane domains (denoted 1–751 NKCC1; Fig. 2). Injection of synthetic mRNA encoding 1–751 NKCC1 resulted in partial secondary axis induction in 62% of embryos ($n = 65$). Since all three NKCC1 constructs were capable of inducing secondary axes, we conclude that there are at least two separable secondary axis-inducing activities: 1–751 and the C-terminal domain 1079–1166. As 1079–1166 NKCC1, which lacks all transmembrane domains that constitute the core of co-transporter, has axis-inducing activity, these results suggest that co-transporter function is dispensable for this activity.

The NKCC1-induced secondary axes lacked heads, but were otherwise properly organized, as shown by the presence of organized dorsal axial tissue, skeletal muscle (Fig. 2*F*). This phenotype is indicative of Bone Morphogenetic Protein (BMP) antagonism or weak activation of Wnt signalling. We found that in animal cap explants FL NKCC1 could induce very low levels of expression of *Siamois*, a direct transcriptional target of

canonical Wnt signalling in *Xenopus* embryos (Carnac *et al.* 1996) (Fig. 3*A*). For comparison, moderate stimulation of the Wnt pathway by LiCl (0.1 M for 5 min) induces much greater levels of *Siamois* mRNA expression (Fig. 3*A*). We believe that the barely detectable activation of *Siamois* by NKCC1 is not consistent with its prominent axis-inducing activity. To directly test whether secondary axis-inducing activity of NKCC1 requires canonical Wnt signalling, we co-expressed FL NKCC1 with dominant-negative *Xenopus* Tcf3 (ΔTcf3), which blocks the canonical Wnt pathway in the nucleus (Molenaar *et al.* 1996). As shown in Fig. 3*D* and *E*, ΔTcf3 had no effect on secondary axis-inducing activity of NKCC1, but was otherwise functional, as assessed by its axis-interfering activity (head loss) upon anterior injection (Fig. 3*G*). Taken together these results strongly suggest that NKCC1 activity in *Xenopus* embryos does not rely on the Wnt/$\beta$-catenin pathway.

### NKCC1 induces neural tissue in animal pole explants from *Xenopus* embryos

We next examined the possibility that NKCC1 acts by antagonizing BMP, as BMP antagonism is known to induce partial secondary axes in *Xenopus* embryos (Zimmerman *et al.* 1996). Animal caps (embryonic ectoderm, which develops into epidermis when cultured in isolation) were explanted at the blastula stage from embryos over-expressing NKCC1 variants and cultured until stage control sibling embryos reached early tadpole stages. Animal caps exposed to BMP antagonists are known to develop neural tissue instead of adopting epidermal fate (De Robertis & Kuroda, 2004). The neural tissue induced by BMP antagonists in animal caps is of anterior character, and this can be readily observed by appearance of the cement gland, which is a structure that marks the anterior-most part of *Xenopus* tadpoles. As shown in

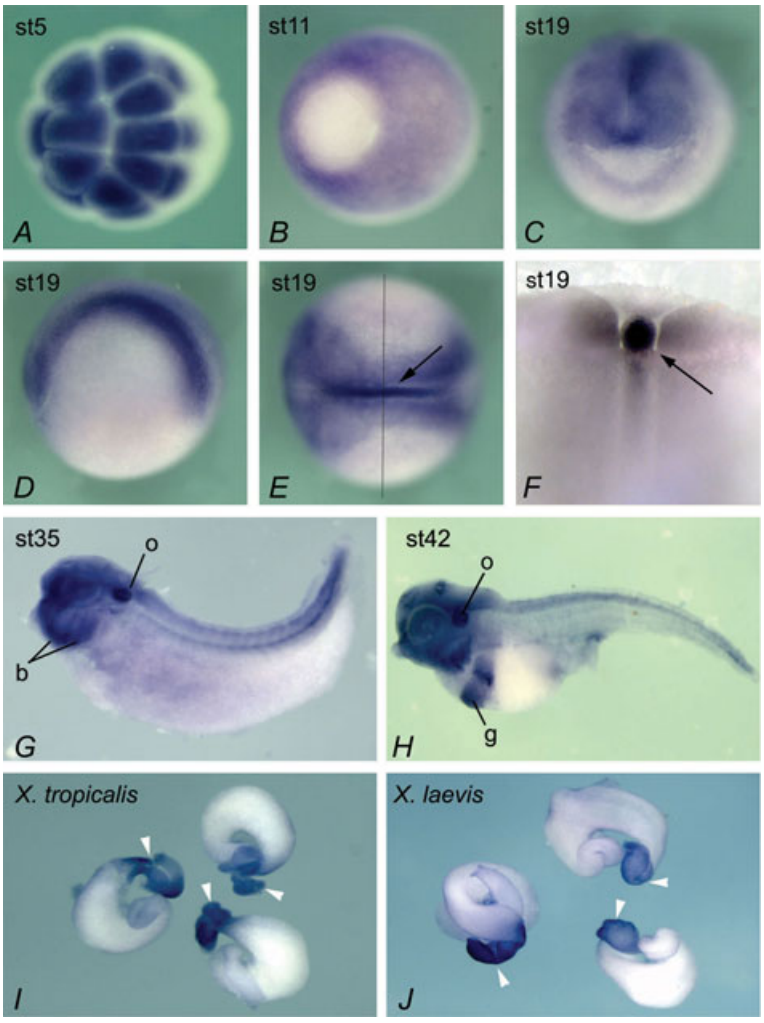


**Figure 1. Expression of NKCC1 in *Xenopus* embryos**
Animal pole view at stage 5, showing high levels of maternal NKCC1 mRNA (*A*). Vegetal view at gastrula stage 11, with prominent expression in ectoderm. Vegetal pole (embryonic endoderm) shows very little NKCC1 staining (*B*). Frontal view of stage 19 embryo, showing NKCC1 expression in developing nervous system (*C*). Lateral view at stage 19, anterior to the left (*D*). Dorsal view at the same stage, showing high levels of NKCC1 mRNA in neural tissue and the notochord (arrow), and lower level of expression in non-neural ectoderm (*E*). An embryo in *E* was dissected along the indicated line, to confirm strong expression of NKCC1 in the notochord and additionally show expression in adjacent somites (*F*). At tadpole stages 35 in *G* and 42 in *H*, NKCC1 continues to be widely expressed, with higher levels of RNA detected in the otic vesicle (o), branchial arches (b) and gut (g). Dorsal is up, and anterior is to the left. Dissected guts at stage 54 from *X. tropicalis* (*I*) and *X. laevis* (*J*). White arrowheads indicate stomach.

Fig. 4, NKCC1 induced the formation of cement gland-like structures. This observation was confirmed by RT-PCR analysis of the cement gland marker XAG (Gammill & Sive, 1997). XAG transcripts were found to be present in animal cap explants that over-expressed either FL NKCC1 or 1079–1166 NKCC1 (Fig. 4). As the cement gland is not of neural origin, to investigate whether NKCC1 induced neural tissue in explants, expression of the neural marker N-tubulin was analysed (Richter *et al.* 1988). As can be seen in Fig. 4, over-expression of each of the NKCC1 constructs individually in animal cap explants resulted in induction of N-tubulin, indicating that all three NKCC1 constructs are capable of inducing the formation of neural tissue in animal cap explants.

Neural specification in the developing *Xenopus* embryo, and more generally in vertebrates, requires inhibition of BMP signalling. Our finding that NKCC1 induces neural tissue in ectodermal explants suggests that it has BMP-antagonizing activity.

It has been shown that MAPK signalling can contribute to neural induction by inhibiting the BMP signalling pathway at the level of *Smad*1 (Sater *et al.* 2003; Kuroda *et al.* 2005). Since Panet *et al.* (2006) have previously reported that NKCC1 may activate ERK in Balb/c 3T3 fibroblasts, we considered whether NKCC1 may antagonize BMP by activation of ERK. However, we found that NKCC1 does not cause significant activation of ERK in animal cap explants (data not shown), arguing that activation of ERK is unlikely to be a major contributor to activities of NKCC1 in *Xenopus*.

### The co-transporter activity is not required for secondary axis induction by NKCC1

Our results have suggested that NKCC1 does not use its co-transporter activity to induce secondary axes upon over-expression in *Xenopus* embryos, as the induction of secondary axes was also observed with the C-terminal fragment that lacked the transmembrane domains required for ion transport activity. However, to directly test whether co-transporter activity was required for the induction of secondary axes in embryos over-expressing NKCC1 we used bumetanide and furosemide, which are well-described soluble inhibitors of SLC12 co-transporters. In *Xenopus* 10 $\mu$M or 500 $\mu$M bumetanide and 2 mM furosemide have been used previously (Suvitayavat *et al.* 1994; Mercado *et al.* 2001). We used a range of concentrations above and below these to ensure blocking the co-transporter function of NKCC1. Bumetanide was used within the range of 5 $\mu$M

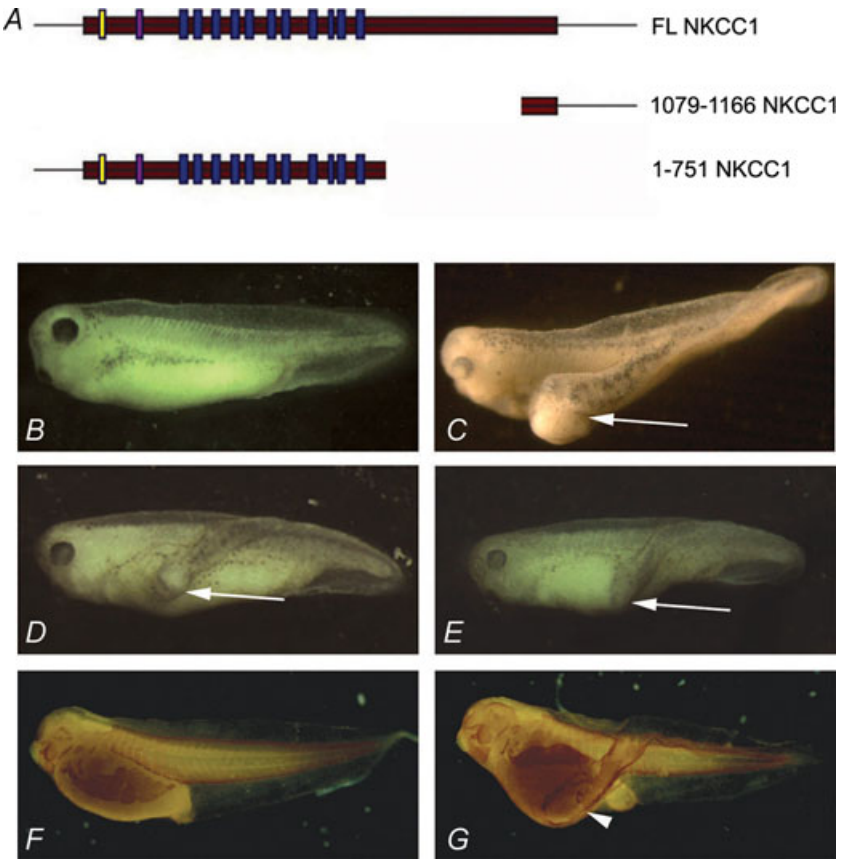


**Figure 2. Injection of NKCC1 mRNA in one posterior blastomere at 4-cell stage *Xenopus laevis* embryos induces partial secondary axis**
*A*, schematic diagram representing the three NKCC1 constructs: full length NKCC1 (FL NKCC1), a C-terminal deletion construct of 410 amino acids (1–751 NKCC1) and a heavily truncated form encompassing only 87 amino acids of the C-terminus (1079–1166 NKCC1). *B*, uninjected control embryo. *C*, injection of 4 ng N-terminal truncated NKCC1 (1079–1166 NKCC1) mRNA induces partial secondary axis (white arrow) in 48% of injected embryos ($n = 87$). *D*, injection of 800 pg full length NKCC1 (FL NKCC1) mRNA induces partial secondary axis (white arrow) in 45% of injected embryos ($n = 87$). *E*, injection of 800 pg C-terminal truncated NKCC1 (1–751 NKCC1) mRNA induces partial secondary axis (white arrow) in 62% of injected embryos ($n = 65$). *F* and *G*, staining with skeletal muscle-specific 12/101 antibody. *F*, uninjected control embryo at stage 33. *G*, 1079–1166 NKCC1 injected embryo at stage 33. White arrowhead indicates ectopic skeletal muscle present in secondary axis.

**Table 1. Bumetanide and furosemide do not affect secondary axis-inducing activity of NKCC1**

| | NAM | NAM + bumetanide (0.9 mM) | NAM + furosemide (2 mM) |
|---|---|---|---|
| Uninjected controls | 0% ($n = 67$) | 0% ($n = 61$) | 0% ($n = 47$) |
| FL NKCC1 | 32% ($n = 59$) | 36% ($n = 61$) | 29% ($n = 55$) |
| 1079–1166 NKCC1 | 32% ($n = 62$) | 35% ($n = 65$) | 32% ($n = 60$) |

Four nanograms of 1079–1166 NKCC1 or 800 pg of FL NKCC1 mRNAs were injected in one ventral blastomere at the 4-cell stage, and the embryos were scored for secondary axes 2.5 days later at stage 35. NAM, normal amphibian media. Furosemide and bumetanide were added to the media 2 h after injection (the same results were observed if the inhibitors were present from the time of injection).

to 1.1 mM. Furosemide was used in the range of 0.5 mM to 3 mM. Neither of the inhibitors blocked the induction of secondary axes in embryos injected with the FL or 1079–1166 NKCC1 mRNA (see Table 1).

To confirm that the secondary axis-forming ability of NKCC1 is not dependent upon its carrier activity, the sodium or the chloride ions from the incubation media, which are required for co-transporter activity, were replaced with choline or isethionic acid, respectively. Neither replacement media inhibited the induction of secondary axes by over-expression of FL NKCC1 or 1079–1166 NKCC1 (Table 2), confirming that the secondary axis-inducting capability of NKCC1 is independent of its co-transporter function.

## Discussion

*Xenopus* NKCC1 is an 11 transmembrane domain protein that is syntenic with its mammalian orthologues. The expression of NKCC1 is first detected as maternal mRNA

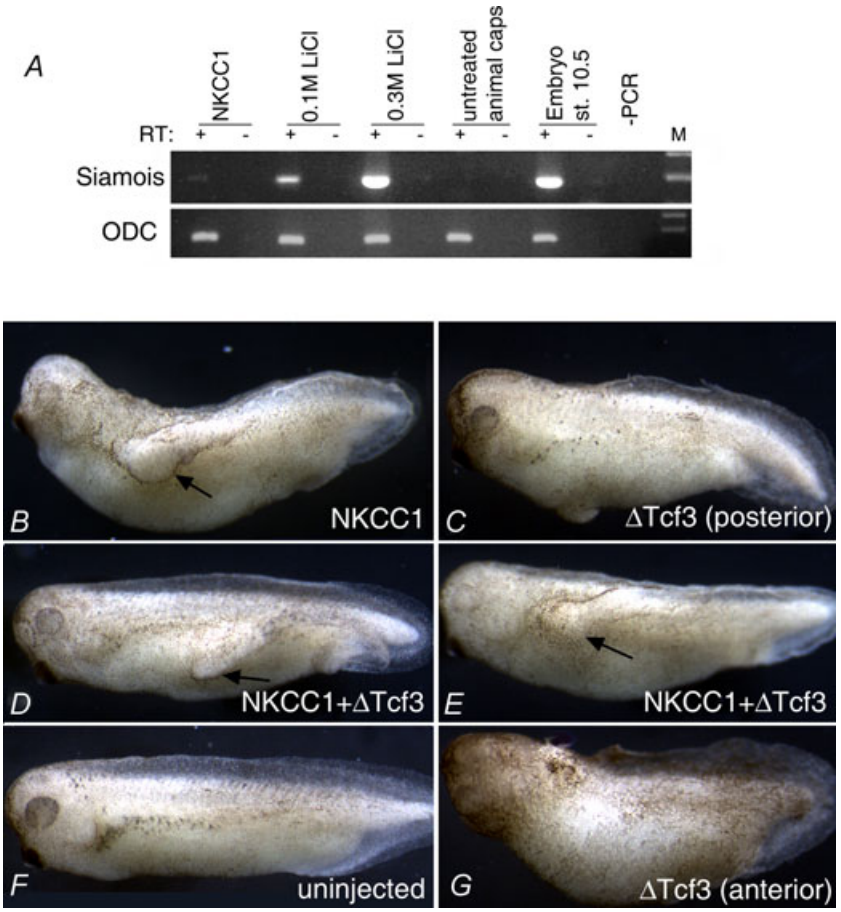


**Figure 3. NKCC1 is a poor inducer of *Siamois* and it does not require Wnt/β-catenin signalling to induce secondary axis in *Xenopus* embryos**
*A*, RT-PCR analyses of *Siamois* expression in animal pole explants treated as indicated. 800 pg of FL NKCC1 was injected into 1- or 2-cell stage embryos. Weak or strong activation of Wnt pathway was achieved by LiCl treatment (see Methods). Explants were collected when sibling control embryos reached stage 10.5, approximately 3 h after excision, a time point which is appropriate for rapid activation of a direct target. Ornithine decarboxylase (ODC) expression was used as a loading control. RT + or – indicates the presence or absence of reverse transcriptase in samples. *B–E*, embryos were injected into one posterior blastomere or two anterior blastomeres (*G*) with indicated mRNAs. 800 pg of NKCC1 and 300 pg of ΔTcf3 was used. The injection of NKCC1 alone induces secondary axes in 50% ($n = 22$) of embryos (*B*), and this activity is not reduced by coinjection of ΔTcf3 (61% of secondary axes; $n = 41$) (*D* and *E*). ΔTcf3 used in this experiment is active, as it causes axis truncation upon anterior injection (*G*).

**Table 2. Secondary axis-inducing activity of NKCC1 does not require $Na^+$ or $Cl^-$ ion flux**

| | MMR | MMR – $Na^+$ | MMR – $Cl^-$ |
|---|---|---|---|
| Uninjected controls | 0% ($n = 40$) | 0% ($n = 36$) | 0% ($n = 37$) |
| FL NKCC1 | 36% ($n = 30$) | 36% ($n = 31$) | 30% ($n = 30$) |
| 1079–1166 NKCC1 | 27% ($n = 34$) | 24% ($n = 33$) | 28% ($n = 31$) |

MMR media with indicated modifications (see Methods) was used to incubate embryos injected with 4 ng of 1079–1166 NKCC1 or 800 pg of FL NKCC1 mRNAs in one ventral blastomere at the 4-cell stage, and the embryos were scored for secondary axes 2.5 days later at stage 35.

in the animal pole of early cleavage stage embryos. The zygotic mRNA is initially expressed nearly uniformly at low levels. From neurula stages, higher levels of expression are observed in distinct structures including neural tissue, kidney, otic vesicle and in later tadpole stages in stomach, similarly to expression patterns that have been reported in other species (Payne & Forbush, 1995; Delpire *et al.* 1999; Dixon *et al.* 1999; Kanaka *et al.* 2001). In addition, *Xenopus* NKCC1 is strongly expressed in the notochord, whose cells have distinct apico-basal polarity. NKCC1 is known to be involved in basolateral secretion is several tissues, including the intestine and stomach, specifically in $Cl^-$ uptake, and this is consistent with strong expression of the NKCC1 transcript in these organs. NKCC1 is also thought to have a role in the inner ear as mutations of NKCC1 in mice lead to deafness (Delpire *et al.* 1999). We have shown that NKCC1 is highly expressed in the otic vesicle of the *Xenopus* embryo, thus suggesting a conserved role for NKCC1 in the development of inner ear.

*Xenopus* NKCC1 was identified in an expression screen for secondary axis-inducing activities. NKCC1 induces incomplete (headless) secondary axes. Several pathways are known to be able to induce incomplete ectopic embryonic axes, including weak activation of the Wnt pathway and BMP antagonism. We found that NKCC1 does not require activation of the Wnt/$\beta$-catenin pathway to induce secondary axes in *Xenopus* embryos, as this activity is not inhibited by $\Delta$Tcf3, a dominant-negative version of an essential nuclear mediator of canonical Wnt signalling. However, we have also found that NKCC1 can very weakly activate the Wnt pathway in animal cap explants, and therefore at present we cannot completely exclude the possibility that this activity contributes to other activities of NKCC1 in *Xenopus* embryos.

In contrast to very weak activation of the Wnt target gene *Siamois,* NKCC1 readily induced neural and cement gland tissue in ectodermal explants (Fig. 4). Since the induction of these tissues requires inhibition of BMP signalling, these results suggest that the activities of NKCC1 in *Xenopus* gain-of-function assays may be mediated by BMP antagonism. Whether and how NKCC1 modulates BMP signalling will be the subject of future work

Our results demonstrate that NKCC1 has at least two separable secondary axis-inducing domains, contained within amino acids 1079–1166 and 1–751. These

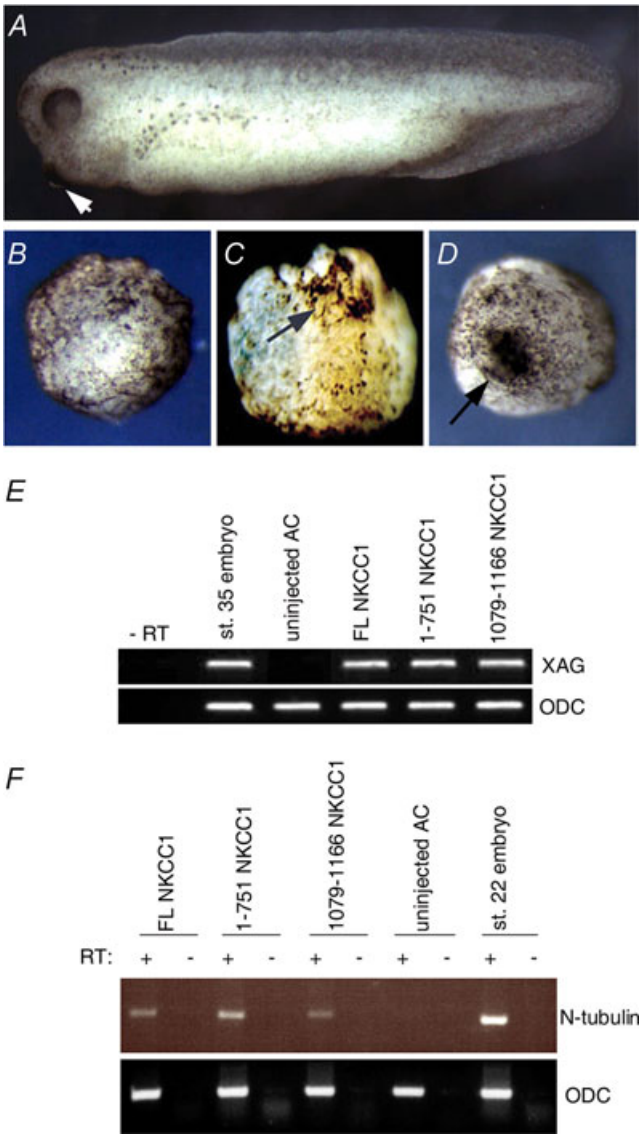


**Figure 4. Injection of NKCC1 mRNA in animal explants induces cement glands and neural tissue formation**
*A*, sibling stage control embryo (stage 35). *B*, uninjected control animal cap (stage 35). *C*, injection of 4 ng of N-terminal truncated NKCC1 (1079–1166 NKCC1) mRNA or, *D*, of 800 pg full length NKCC1 (FL NKCC1) mRNA induces cement gland formation in animal cap explants. Arrows point to cement glands. *E*, over-expression of FL NKCC1, 1–751 NKCC1 and 1079–1166 NKCC1 causes expression of XAG cement gland marker in animal cap explants. RT-PCR analyses were carried out on stage 35 animal cap explants, and sibling stage control embryos served as positive control. ODC RT-PCR was used as a loading control. *F*, injection of either full length NKCC1, 1–751 NKCC1 or 1079–1166 NKCC1 induces expression of neural marker N-tubulin in animal explants, as assessed by RT-PCR. RT + or – indicates the presence or absence of reverse transcriptase in samples.

results imply that NKCC1 is inducing secondary axes independently of its co-transporter role. To directly examine if NKCC1 requires its co-transporter activity to induce secondary axes upon over-expression, bumetanide and furosemide, two well-described NKCC co-transporter inhibitors were used. We also removed $Na^+$ and reduced $Cl^-$ ions from the media that injected embryos were cultured in, since transport of these ions is known to be required for co-transporter activity of NKCC1. Neither the inhibitor treatment nor media replacement had any effect on the ability of NKCC1 to induce secondary axis formation (Tables 1 and 2), leading us to conclude that secondary axis formation is induced by NKCC1 independently of its co-transporter role.

As mentioned above, given that the 1079–1166 NKCC1 construct, which lacks all transmembrane domains, is active in our assays, this result is perhaps not surprising. However, the lack of effect of bumetanide, furosemide and ion replacement also indicates that all NKCC1 variants tested, including the 87 amino-acid C-terminal fragment, do not work by modulating the co-transporter activity of endogenous NKCC transporters. Future work will address the molecular mechanism by which NKCC1 acts in *Xenopus* embryo assays, including the possibilities of competitive inhibition of an enzyme, perhaps a kinase, or modulation of activity of other membrane proteins.

### Conclusions

The main finding of this report is that NKCC1 can induce secondary axes and neural tissue in *Xenopus* embryos upon over-expression. Our evidence suggests that this activity does not require co-transporter activity of NKCC1, implying that NKCC1 has other roles in addition to ion transport.

## References


Carnac G, Kodjabachian L, Gurdon JB & Lemaire P (1996). The homeobox gene Siamois is a target of the Wnt dorsalisation pathway and triggers organiser activity in the absence of mesoderm. *Development* **122**, 3055–3065.

Chomczynski P & Sacchi N (1987). Single-step method of RNA isolation by acid guanidinium thiocyanate-phenol-chloroform extraction. *Anal Biochem* **162**, 156–159.

Darman RB, Flemmer A & Forbush B (2001). Modulation of ion transport by direct targeting of protein phosphatase type 1 to the Na-K-Cl cotransporter. *J Biol Chem* **276**, 34359–34362.

De Robertis EM & Kuroda H (2004). Dorsal-ventral patterning and neural induction in *Xenopus* embryos. *Annu Rev Cell Dev Biol* **20**, 285–308.

Delpire E, Lu J, England R, Dull C & Thorne T (1999). Deafness and imbalance associated with inactivation of the secretory Na-K-2Cl co-transporter. *Nat Genet* **22**, 192–195.

Dixon MJ, Gazzard J, Chaudhry SS, Sampson N, Schulte BA & Steel KP (1999). Mutation of the Na-K-Cl co-transporter gene *Slc12a2* results in deafness in mice. *Hum Mol Genet* **8**, 1579–1584.

Flatman PW (2002). Regulation of Na-K-2Cl cotransport by phosphorylation and protein–protein interactions. *Biochim Biophys Acta* **1566**, 140–151.

Flatman PW (2008). Cotransporters, WNKs and hypertension: an update. *Curr Opin Nephrol Hypertens* **17**, 186–192.

Gamba G (2005). Molecular physiology and pathophysiology of electroneutral cation-chloride cotransporters. *Physiol Rev* **85**, 423–493.

Gamba G, Miyanoshita A, Lombardi M, Lytton J, Lee WS, Hediger MA & Hebert SC (1994). Molecular cloning, primary structure, and characterization of two members of the mammalian electroneutral sodium-(potassium)-chloride cotransporter family expressed in kidney. *J Biol Chem* **269**, 17713–17722.

Gamba G, Saltzberg SN, Lombardi M, Miyanoshita A, Lytton J, Hediger MA, Brenner BM & Hebert SC (1993). Primary structure and functional expression of a cDNA encoding the thiazide-sensitive, electroneutral sodium-chloride cotransporter. *Proc Natl Acad Sci U S A* **90**, 2749–2753.

Gammill LS & Sive H (1997). Identification of otx2 target genes and restrictions in ectodermal competence during Xenopus cement gland formation. *Development* **124**, 471–481.

Garg P, Martin CF, Elms SC, Gordon FJ, Wall SM, Garland CJ, Sutliff RL & O'Neill WC (2007). Effect of the Na-K-2Cl cotransporter NKCC1 on systemic blood pressure and smooth muscle tone. *Am J Physiol Heart Circ Physiol* **292**, H2100–H2105.

Gilchrist MJ, Zorn AM, Voigt J, Smith JC, Papalopulu N & Amaya E (2004). Defining a large set of full-length clones from a *Xenopus* tropicalis EST project. *Dev Biol* **271**, 498–516.

Gimenez I (2006). Molecular mechanisms and regulation of furosemide-sensitive Na-K-Cl cotransporters. *Curr Opin Nephrol Hypertens* **15**, 517–523.

Hebert SC, Mount DB & Gamba G (2004). Molecular physiology of cation-coupled $Cl^-$ cotransport: the SLC12 family. *Pflugers Arch* **447**, 580–593.

Kanaka C, Ohno K, Okabe A, Kuriyama K, Itoh T, Fukuda A & Sato K (2001). The differential expression patterns of messenger RNAs encoding K-Cl cotransporters (KCC1,2) and Na-K-2Cl cotransporter (NKCC1) in the rat nervous system. *Neuroscience* **104**, 933–946.

Kintner CR & Brockes JP (1984). Monoclonal antibodies identify blastemal cells derived from dedifferentiating limb regeneration. *Nature* **308**, 67–69.

Kuroda H, Fuentealba L, Ikeda A, Reversade B & De Robertis EM (2005). Default neural induction: neuralization of dissociated *Xenopus* cells is mediated by Ras/MAPK activation. *Genes Dev* **19**, 1022–1027.

Liedtke CM & Cole TS (2002). Activation of NKCC1 by hyperosmotic stress in human tracheal epithelial cells involves PKC-d and ERK. *Biochim Biophys Acta* **1589**, 77–88.

Lytle C (1997). Activation of the avian erythrocyte Na-K-Cl cotransport protein by cell shrinkage, cAMP, fluoride, and calyculin-A involves phosphorylation at common sites. *J Biol Chem* **272**, 15069–15077.

Mercado A, de los Heros P, Vazquez N, Meade P, Mount DB & Gamba G (2001). Functional and molecular characterization of the K-Cl cotransporter of *Xenopus laevis* oocytes. *Am J Physiol Cell Physiol* **281**, C670–C680.

Molenaar M, van de Wetering M, Oosterwegel M, Peterson-Maduro J, Godsave S, Korinek V, Roose J, Destree O & Clevers H (1996). XTcf-3 transcription factor mediates beta-catenin-induced axis formation in *Xenopus* embryos. *Cell* **86**, 391–399.

Nieuwkoop PD & Faber J (1994). *Normal Table of Xenopus laevis (Daudin): a Systematical and Chronological Survey of the Development from the Fertilized Egg Till the End of Metamorphosis*. Garland Publications, New York, London.

Panet R, Eliash M & Atlan H (2006). $Na^+/K^+/Cl^-$ cotransporter activates MAP-kinase cascade downstream to protein kinase C, and upstream to MEK. *J Cell Physiol* **206**, 578–585.

Payne JA & Forbush B 3rd (1995). Molecular characterization of the epithelial Na-K-Cl cotransporter isoforms. *Curr Opin Cell Biol* **7**, 493–503.

Piechotta K, Lu J & Delpire E (2002). Cation chloride cotransporters interact with the stress-related kinases Ste20-related proline-alanine-rich kinase (SPAK) and oxidative stress response 1 (OSR1). *J Biol Chem* **277**, 50812–50819.

Richter K, Grunz H & Dawid IB (1988). Gene expression in the embryonic nervous system of *Xenopus laevis*. *Proc Natl Acad Sci U S A* **85**, 8086–8090.

Sater AK, El-Hodiri HM, Goswami M, Alexander TB, Al-Sheikh O, Etkin LD & Akif Uzman J (2003). Evidence for antagonism of BMP-4 signals by MAP kinase during *Xenopus* axis determination and neural specification. *Differentiation* **71**, 434–444.

Sive HL, Grainger RM & Harland RM (2000). *Early Development of Xenopus laevis: a Laboratory Manual*. Cold Spring Harbor Laboratory Press, Cold Spring Harbor, New York.

Suvitayavat W, Dunham PB, Haas M & Rao MC (1994). Characterization of the proteins of the intestinal $Na^+$-$K^+$-$2Cl^-$ cotransporter. *Am J Physiol Cell Physiol* **267**, C375–C384.

Xu JC, Lytle C, Zhu TT, Payne JA, Benz E Jr & Forbush B 3rd (1994). Molecular cloning and functional expression of the bumetanide-sensitive Na-K-Cl cotransporter. *Proc Natl Acad Sci U S A* **91**, 2201–2205.

Zimmerman LB, De Jesus-Escobar JM & Harland RM (1996). The Spemann organizer signal noggin binds and inactivates bone morphogenetic protein 4. *Cell* **86**, 599–606.

## Acknowledgements

This study was supported by the Association for International Cancer Research. The 12/101 antibody was obtained from the Developmental Studies Hybridoma Bank developed under the auspices of the NICHD and maintained by The University of Iowa, Department of Biological Sciences, Iowa City, IA 52242, USA. We are grateful to Dr Daniela Riccardi for suggesting the media replacement experiment and for critical reading of the manuscript.

## Author's present address

Z. S. Walters: Institute of Cancer Research, Sutton, Surrey, SM2 5NG, UK.